

1 Revision 2

2 **The fate of ammonium in phengite during high temperature**

3 **processes**

4 YAN YANG^{1,*}, VINCENT BUSIGNY², ZHONGPING WANG³, QUNKE XIA¹

5 ¹ Institute of Geology and Geophysics, School of Earth Sciences, Zhejiang University, Hangzhou
6 310027, China

7 ² Institut de Physique du Globe de Paris, Sorbonne Paris Cité, University Paris Diderot, UMR
8 7154 CNRS, F-75005 Paris, France

9 ³ Physics Experiment Teaching Center, University of Science and Technology of China, Hefei
10 230026, China

11 * Corresponding author

12 Institute of Geology and Geophysics

13 School of Earth Sciences

14 Zhejiang University

15 Hangzhou 310027, China

16 Email: yanyang2005@zju.edu.cn

17 **ABSTRACT**

18 Nitrogen (N) is the main component of the atmosphere and is largely considered
19 as a volatile element. However, most researchers now agree that a significant amount
20 of N, in the form of ammonium (NH₄⁺) substituting for K⁺ in some K-bearing
21 minerals such as clays, micas, and feldspars, can be transferred to the deep Earth
22 through subduction. The fate of ammonium in those minerals during subduction is
23 still poorly known but is likely controlled by temperature and pressure pathways. In
24 an attempt to contribute to understanding the fate of N during high temperature
25 processes, we carried out *in situ* high temperature IR and Raman spectra
26 measurements to investigate the rate and mechanism of NH₄⁺ loss in phengite. We
27 observed that a new OH band at 3425 cm⁻¹ became prominent above 400 °C, and did
28 not change with times during isothermal annealing at 500 and 700 °C. The N-H
29 stretching band shifted to higher wavenumbers in the temperature interval from -150
30 to 20 °C, while linearly shifted to lower wavenumbers in the temperature interval
31 from 20 to 500 °C and remained stable above 500 °C. The N-H bending band linearly
32 shifted to lower wavenumbers in the temperature interval from -150 to 400 °C and

33 remained stable. The K-O stretching frequency decreased with increasing temperature
34 to 600 °C, and then remained stable. These processes were reversible until
35 dehydration and ammonium loss from phengite starting at 800 °C. The results suggest
36 that (1) at low temperatures, ammonium is ordered and hydrogen bonding between
37 ammonium and the framework evolves during cooling; (2) at high temperatures, the
38 N-H interatomic distance of NH_4^+ lengthens with increasing temperature until 500 °C.
39 N-H bond subsequently no longer lengthens, accompanied by H transferring from N
40 to neighboring O and forming a new OH band at 3425 cm^{-1} . At 800 °C, H^+ starts
41 breaking from N and leaving others to form NH_3 and OH^- . This study has implications
42 for evaluating the extent to which these minerals can preserve information regarding
43 nitrogen behavior during high temperature processes.

44 **Keywords:** phengite, nitrogen, ammonium, high temperature, IR, Raman

45 INTRODUCTION

46 Nitrogen (N) is an essential element for all living organisms. Although N is one
47 of the predominant elements in the atmosphere and biosphere on Earth surface, it only
48 accounts for 25–30% of the total planet inventory. Large amounts of N indeed reside
49 in the deep Earth (Galloway 2003; Goldblatt et al. 2009; Palya et al. 2011; Busigny
50 and Bebout 2013; Johnson and Goldblatt 2015). In sedimentary rocks, N occurs
51 essentially as ammonium (NH_4^+) released from decomposed organic matter and is
52 substituted for K^+ in some K-bearing minerals such as clays, micas, and feldspars
53 (Williams et al. 1992). A significant amount of N, in the form of NH_4^+ , can then be
54 transferred to the deep Earth reservoir through subduction. The speciation of N in the
55 Earth mantle is not very well constrained due to the very low N concentration and the
56 poor degree of preservation of mantle rocks recovered at the surface (Yokochi et al.
57 2009). However, several recent theoretical and experimental studies suggested that
58 NH_4^+ may be the main N species in most of the mantle (Watenphul et al. 2010; Li et al.
59 2013; Mikhail and Sverjensky 2014).

60 To address the N cycle in the deep Earth, extensive works have concerned the

61 size and isotope composition of major crustal and upper-mantle N reservoirs (e.g.,
62 Cartigny and Marty 2013 and references therein; Halama et al. 2014; Li et al. 2014).
63 Recently, some studies reported N solubility in high-pressure minerals typical of deep
64 Earth conditions (Li et al. 2013; Watenphul et al. 2009, 2010; Nobel 2016). Since
65 subduction is the important mechanism for carrying N into deep reservoirs, it is
66 crucial to determine the extent to which minerals can preserve NH_4^+ during deep
67 subduction. Studies on sediments subducted to different depths show either a decrease
68 or a preservation of N concentration with increasing metamorphic grade (Bebout and
69 Fogel 1992; Mingram and Bräuer 2001; Busigny et al. 2003a; Plessen et al. 2010).
70 One of the most important parameters for N stability or loss in subducting rocks was
71 suggested to be the geothermal gradient, specifically temperature variations (Bebout
72 et al. 1999a; Busigny et al. 2003a; Busigny and Bebout 2013). However, the diffusion
73 rate and mechanism of NH_4^+ loss in the host minerals such as micas, alkali feldspar
74 and clinopyroxene are still poorly known. Several studies have compared the rates of
75 NH_4^+ loss and dehydration in some minerals, but there is still no consensus on rate
76 and mechanism of NH_4^+ loss. For example, Higashi (1978, 2000) suggested that NH_4^+
77 loss was far ahead of dehydration in sericite (a fine grained variety of muscovite with
78 chemical formula $\text{K}(\text{AlFeMg})_2(\text{SiAl})_4\text{O}_{10}(\text{OH})_2.n\text{H}_2\text{O}$) based on differential thermal
79 analysis. Other works argued that in NH_4 -analcime, NH_4^+ loss and dehydration were
80 parallel processes based on thermogravimetric and Fourier Transform Infrared (FTIR)
81 spectrometry analyses (Miroshnichenko and Drebuschak 2003; Likhcheva et al.
82 2004). Using *in situ* high temperature FTIR spectra, Zhang et al. (2010) suggested that
83 NH_4^+ loss in muscovite happened at temperatures near dehydration.

84 Phengite is the most common high-pressure white mica observed in subducted
85 metasediments. Experimental works indicated that phengite was stable and could
86 carry water to depths of about 300 km in subduction environment (Poli and Schmidt
87 1995; Domanik and Holloway 1996; Schmidt 1996; Schmidt and Poli 1998, 2014).
88 Busigny et al. (2003b) reported that phengite from Western Italian Alps contained
89 high NH_4^+ concentrations (up to 2000 ppm) in metasediments subducted down to ~90

90 km depth (3 GPa). Thus NH_4^+ -bearing phengite represents an important component
91 for N and H transfer to the deep mantle (Watenphul et al. 2009; Bebout et al. 2016).

92 Since NH_4^+ substitutes for K^+ in the phengite structure, knowledge of evolutions
93 of N-H bond and its host lattice at high temperature are necessary to understand the
94 stability of NH_4^+ during the recycling process into the deep Earth. In the present study,
95 we carried out *in situ* high temperature FTIR and Raman spectroscopic investigations
96 of NH_4^+ and lattice framework in phengite respectively, and analyze their behavior at
97 high temperature. We explored the temperature dependence of N-H and K-O length,
98 and further figured out the rate and mechanism of NH_4^+ loss in phengite. The results
99 have implications for better understanding the fate of ammonium in phengite during
100 high-temperature processes.

101 MATERIALS AND METHODS

102 Sample description

103 Phengite crystals from a natural sample were used here as a starting material.
104 They were extracted from a single high-pressure metasediment of the western Alps
105 (sample 98SE8). This sample was characterized in a previous study (Busigny et al.,
106 2003b) and was selected for its high NH_4^+ content (~2000 ppm) in phengite, thus
107 allowing relatively easy measurement by IR spectroscopy. The phengite powder was
108 used for the X-ray diffraction measurement. Intensity data were collected using $\text{CuK}\alpha$
109 radiation with 2θ ranging from 3 to 70° . Based on the X-ray diffraction analysis (see
110 supplementary material), this sample is trigonal. The unit-cell parameters of the
111 sample are as following: $a = 5.225 \text{ \AA}$, $b = 5.225 \text{ \AA}$, $c = 29.75 \text{ \AA}$, $\alpha = \beta = 90^\circ$, $\gamma = 120^\circ$.
112 Figure 1 illustrates where ammonium is substituting into the phengite structure. The
113 average chemical composition of the sample 98SE8 was reported in Busigny et al.
114 (2003b): 55.6% SiO_2 , 0.07% TiO_2 , 21.03% Al_2O_3 , 4.48% FeO , 0.05% MnO , 4.42%
115 MgO , 0.00% CaO , 0.04% Na_2O . The size of the crystals ranged between 0.2 and 2
116 mm. The thickness of the analyzed grains ranged from 0.01 to 0.12 mm.

117 Low and high temperature FTIR spectroscopy

118 For the *in situ* low temperature measurement, the phengite sample was placed on
119 an Al foil with a hole of 1.5 mm in diameter in a Linkam FTIR600 heating/cooling
120 stage with ZnSe windows. The temperature step was regulated by a Linkam TMS94
121 controller with 0.1 °C accuracy. The sample was cooled successively from room
122 temperature to 0 °C, -50 °C, -100 °C and -150 °C at a cooling rate of 10 °C/min. For
123 every temperature step, the dwell time was 10 minutes.

124 For the *in situ* high temperature measurement, the phengite sample was placed on
125 a Pt foil with a hole of 1.5 mm in diameter in an Instec HS1300 heating stage with
126 CaF₂ windows, equipped with a resistance heater and an S type thermocouple. The
127 sample was heated in Ar and air, respectively. The sample temperature was
128 determined with a typical uncertainty of less than 1 °C. The temperature was initially
129 increased from 20 to 100 °C, and then by 100 °C increments to 800 °C, using a heating
130 rate of 15 °C/min. For every temperature step, the dwell time was 5 minutes. The *In*
131 *situ* FTIR measurements in isothermal annealing were conducted using the procedure
132 described by Okumura and Nakashima (2006): the temperature of the heating stage
133 was elevated at a rate of 100 °C /min and held at a desired temperature. After
134 collecting the background FTIR spectrum at the desired temperature, a phengite grain
135 was put in the heating stage and the initial sample FTIR spectrum was measured just
136 after the sample was set.

137 To compare rate of dehydration and ammonium loss, FTIR measurements on
138 quenched samples were conducted. Two thin phengite grains (about 0.01 and 0.03
139 mm thickness) were heated in the heating stage purged with Ar at a desired
140 temperature of 750 and 800 °C for 30 minutes, respectively. Then FTIR measurements
141 were carried out on the samples quenched to room temperature.

142 FTIR spectra in the frequency range 4000-1000 cm⁻¹ were collected with an IR
143 beam direction perpendicular to the (001) plane (i.e. to the layer) using a Nicolet iS50
144 FTIR spectrometer coupled with a Continuum microscope. A KBr beam-splitter and a
145 liquid nitrogen-cooled MCT-A detector were used. A total of 128 scans were
146 accumulated for each spectrum at a 4 cm⁻¹ resolution. The aperture size was set to

147 50×50 μm. Spectra were collected on the same selected area for every sample.

148 ***In situ* high temperature Raman spectroscopy**

149 The phengite sample was placed on a Pt foil in a Linkam TS1500 heating stage,
150 equipped with a resistance heater and an S type thermocouple. The sample
151 temperature was determined with a typical uncertainty of less than 1 °C. The
152 automatic temperature control unit was programmed to set the heating rate at 20
153 °C/min to reach the desired temperature. The dwelling time amounted to 5 minutes at
154 each experimental temperature.

155 *In situ* high temperature Raman spectroscopic analyses were performed with the
156 incident laser beam perpendicular to the (001) plane on a LABRAM-HR spectrometer
157 with 1800 g/mm gratings. Single-crystal silicon was used as a reference. Raman
158 spectra in the frequency range 50-1200 cm⁻¹ were collected at room temperature and
159 from 100 to 800 °C at 100 °C interval. The focal length for the spectrograph was 750
160 mm. The sample was excited by the 514.5 nm green light of a Spectra Physics Ar ion
161 laser. A 50X objective was used to focus the incident laser light on the sample and to
162 collect the scattered light. The diameter of the focused laser light spot was estimated
163 to be 10 μm.

164 **Data analysis**

165 OriginPro 8.0 software was used to analyze IR and Raman spectra at various
166 temperatures.

167 **RESULTS**

168 **FTIR spectra of NH₄⁺ in phengite at room temperature**

169 There are four normal vibrational modes in isolated ammonium: symmetric (ν_1),
170 and antisymmetric (ν_3) stretching vibrations, as well as symmetric (ν_2) and
171 antisymmetric (ν_4) bending vibrations (Herzberg 1966; Kearley and Oxtton 1983). Of
172 these, only ν_3 and ν_4 are IR active. However, for ammonium in a crystal, ν_1 and ν_2
173 bands may appear in IR spectra due to decreased symmetry. FTIR spectroscopy is

174 very sensitive to N-H vibrations and has been used to analyze NH_4^+ in minerals in
175 previous studies (e.g., Busigny et al. 2003b; Watenphul et al., 2009, 2010; Zhang et al.
176 2010; Wunder et al. 2015; Vennari et al. 2016). The polarized and unpolarized IR
177 spectra of NH_4^+ in phengite at room temperature are shown in Figure 2. Following the
178 band assignments from Harlov et al. (2001), Busigny et al. (2003b) and Watenphul et
179 al. (2009) (Table 1), the band at 3291 cm^{-1} corresponds to ν_3 -asymmetric stretching
180 mode while the one at 3036 cm^{-1} reflects a combination of ν_2 -symmetric and
181 ν_4 -antisymmetric bending vibrations. The band at 1430 cm^{-1} corresponds to ν_4 and its
182 corresponding overtone $2\nu_4$ is at 2818 cm^{-1} . Since using an IR beam perpendicular to
183 the (001) plane represents isotropic properties independent from orientation, there is
184 little difference in the absorption of NH_4^+ or OH with the polarizer rotating different
185 angles as shown in Figure 2. Therefore, in the present contribution, we used
186 unpolarized radiation to study ammonium in phengite under different temperatures, as
187 was also applied by Zhang et al. (2010) to study OH and ammonium in muscovite.

188 ***In situ* FTIR spectra of NH_4^+ in phengite at different temperatures**

189 Upon cooling, the bands are intensive, sharp and peak splitting. We can clearly
190 distinguish four new bands at 3219 , 3117 , 2880 and 1404 cm^{-1} as the temperature is
191 decreased down to $-150\text{ }^\circ\text{C}$ (Fig. 3). Those bands are assigned to the vibrations of
192 ammonium (Reed and Williams 2006; Watenphul et al. 2009; Wunder et al. 2015). At
193 high temperatures, changes of the IR spectra with increasing temperature under air
194 and Ar atmospheres are similar, with all bands becoming significantly broad and
195 overlapping (Fig. 4). Most interestingly, a new band at 3425 cm^{-1} becomes prominent
196 above $400\text{ }^\circ\text{C}$. The appearance of this new band is unquenchable, and does not exist in
197 the spectrum at room temperature after heating. The combination of NH_4^+ symmetric
198 and antisymmetric bending band ($\nu_2 + \nu_4$) at 3036 cm^{-1} and the overtone
199 antisymmetric bending band ($2\nu_4$) at 2818 cm^{-1} disappear at $200\text{ }^\circ\text{C}$, while the N-H
200 stretching band (ν_3) at 3291 cm^{-1} and bending band (ν_4) at 1430 cm^{-1} still remain up to
201 $800\text{ }^\circ\text{C}$. The evolution of frequencies of the bands of ν_3 and ν_4 with temperature is
202 plotted in Figure 5. With increasing temperature, the ν_3 band shifts to higher

203 wavenumbers from -150 to 20 °C, while linearly shifts to lower wavenumbers from
204 20 to 500 °C and remains stable above 500 °C. The ν_4 band linearly shifts to lower
205 wavenumbers with increasing temperature from -150 to 400 °C and remains stable.

206 ***In situ* FTIR spectra of NH_4^+ in isothermal annealing and on quenched samples**

207 To investigate the stability of NH_4^+ , we carried out *in situ* FTIR measurements in
208 isothermal annealing at 500 and 700 °C in air, respectively. Figure 6 displays *in situ*
209 IR spectra collected at different time intervals. At the two different temperatures
210 explored herein, the IR absorptions of the new band at 3425 cm^{-1} and ammonium
211 bands do not change with heating times. In addition, the IR spectra are the same at
212 room temperature before and after heating. It should be noted that the weakening of
213 the absorptions at high temperatures compared to room temperature is mainly induced
214 by decreasing absorption coefficient with increasing temperature (e.g., Zhang et al.
215 2007; Tokiwai and Nakashima 2010; Yang et al. 2010, 2012; Radica et al. 2016).

216 We cannot investigate the stability of water in phengite from data presented in
217 Figure 6 since the detector of IR spectrometer is oversaturated for measuring
218 absorption of OH band around 3610 cm^{-1} using the thick sample. To overcome this
219 problem and compare the starting temperature of dehydration and loss of ammonium,
220 we use much thinner samples ($<30\text{ }\mu\text{m}$). We collected IR spectra of the thinner
221 phengite flakes quenched from 750 and 800 °C, respectively (Fig. 7). The absorptions
222 of both OH and NH_4^+ at room temperature before and after heating to 750 °C for 30
223 minutes are almost the same, indicating that water and ammonium in phengite still
224 can be preserved to 750 °C. In contrast, the absorptions of OH and NH_4^+ distinctly
225 decrease comparing the spectra at room temperature before and after heating to
226 800 °C for 30 minutes. The integrated absorptions of NH_4^+ from $2800\text{ to }3400\text{ cm}^{-1}$
227 and $1340\text{ to }1500\text{ cm}^{-1}$ are reduced by 45.8% and 73.1%, respectively, and the
228 integrated absorptions of OH around 3610 cm^{-1} decrease by 25.8%. As a result,
229 dehydration and loss of ammonium in phengite start at the same temperature around
230 800 °C, which supports previous arguments that ammonium loss and dehydration
231 were parallel processes in analcime and muscovite (Miroshnichenko and Drebushchak

232 2003; Likhcheva et al. 2004; Zhang et al. 2010).

233 ***In situ* Raman spectra of lattice vibrations in phengite at high temperatures**

234 Raman spectroscopy is sensitive to local structural environment within crystal
235 and usually used to study lattice vibrations. The Raman spectra of phengite at
236 different temperatures are displayed in the range 50-1200 cm^{-1} (Fig. 8). There are four
237 most prominent bands at 104, 192, 270, and 706 cm^{-1} in the spectrum at room
238 temperature (25 °C). The band assignments are listed in Table 1. Based on lattice
239 dynamic calculations, McKeown et al. (1999) suggested that modes between 800 and
240 360 cm^{-1} had internal tetrahedral sheet motions mixed with K and octahedral Al
241 displacements, and modes at frequencies less than 360 cm^{-1} had lattice motions. In the
242 present study, the band at 104 cm^{-1} is due to K-O stretching vibration according to
243 band assignment of Holtz et al. (1993), McKeown et al. (1999), Mookherjee and
244 Redfern (2002), Zhang et al. (2010) and Williams et al. (2012). Figure 9 displays the
245 mode frequency shifts with temperature. The bands at 192, 270 and 706 cm^{-1} linearly
246 shift to lower Raman frequencies, indicating expansion of the microstructure with
247 increasing temperature. Among these bands, the K-O stretching band at 104 cm^{-1}
248 exhibits interesting temperature dependence. The band frequency decreases with
249 increasing temperature to 600 °C, then remains stable.

250 **DISCUSSION**

251 **The local environment of the ammonium in phengite at low temperature**

252 Pauling (1930) expressed orientational ordering of a tetrahedral molecule such as
253 ammonium and suggested the possibility of a transition from free rotation or tumbling
254 of the ammonium to oscillatory motion on cooling. At room temperature, ammonium
255 freely tumbles and the site symmetry is essentially spherical. Upon cooling, the
256 ammonium freezes into one orientation, multiple equivalent orientations, or hindered
257 oscillation, changing the symmetry with a loss of degeneracy, peak splitting, as well
258 as line narrowing. Mookherjee et al. (2002a and 2002b) observed the peak splitting of
259 ammonium in the IR spectra of tobelite and phlogopite at low temperatures and

260 attributed it to a disorder/order transition of the ammonium. Similarly, the splitting
261 and narrowing IR bands of ammonium during cooling in this study indicates the
262 ordering of ammonium in phengite at low temperatures. Thus a discrete hydrogen
263 bonding between ammonium and the framework evolves at low temperatures. The
264 presence of hydrogen bonding at low temperatures can also be indicated from the
265 lower frequency shift of ν_3 and higher frequency shift of ν_4 (Plumb and Hornig 1955).
266 Figure 5 shows that the frequencies of ν_3 and ν_4 change from 3291 and 1430 cm^{-1} at
267 room temperature to 3286 and 1433 cm^{-1} at $-150\text{ }^\circ\text{C}$, respectively, suggesting the
268 presence of hydrogen bonding at low temperatures.

269 **Origin of the new band at 3425 cm^{-1}**

270 The source of this new band at 3425 cm^{-1} may have two possibilities. First, the
271 NH_3 molecule has four normal modes at 3336 (ν_1), 950 (ν_2), 3444 (ν_3) and 1626 cm^{-1}
272 (ν_4) in the gaseous state (Buback and Schulz 1976). Thus, it may result from the 3444
273 (ν_3) mode of NH_3 . Second, it is due to O-H vibration. In this study, we exclude the
274 first possibility and ascribe it to the O-H vibration based on the following reasons. (1)
275 Ammonium in phengite does not dissociate until 800 $^\circ\text{C}$. Thus the appearance of the
276 new band at 400 $^\circ\text{C}$ is not likely related to NH_3 gas. (2) The IR spectra in this study
277 were recorded from samples heating in open system in air or flushed with Ar. The
278 absorption of the new band does not vary with time during *in situ* isothermal
279 annealing and is not quenchable, which is unlikely for NH_3 gas being very mobile.
280 The new OH band is very weak compared to the original OH band in phengite,
281 indicating it is not the inherent water. Zhang et al. (2010) also observed a new band
282 around 3428 cm^{-1} at 327-427 $^\circ\text{C}$ from the *in situ* high temperature IR spectra of
283 muscovite. They ascribed it to OH resulting from protons migrating to new locations
284 or change of OH environments at the atomic level with increasing temperature.

285 **Evolutions of K-O and ammonium vibrations with temperature**

286 Ammonium locates in the interlayer substituting for K in the phengite (Vedder
287 1965). Thus acknowledgement of high temperature behavior of interlayer is necessary

288 to understand evolutions of ammonium at high temperatures. Considering the
289 relatively low content of ammonium in the sample, the high temperature behavior of
290 the interlayer is likely primarily controlled by K. The Raman spectroscopic study
291 shows the decrease of vibration frequency at 104 cm^{-1} corresponding to K-O vibration
292 with increasing temperature to $600\text{ }^{\circ}\text{C}$. Based on bond length, K-O bond can be
293 divided into $\text{K-O}_{\text{inner}}$ which is shorter and $\text{K-O}_{\text{outer}}$ which is longer (Tateyama *et al.*
294 1977). The band at 104 cm^{-1} was attributed to stretching vibration of $\text{K-O}_{\text{inner}}$
295 (Mookherjee and Redfern 2002; Zhang *et al.* 2010). Thus the decrease of vibration
296 frequency at 104 cm^{-1} with increasing temperature indicates the lengthening of
297 $\text{K-O}_{\text{inner}}$ bond, consistent with the increase in length of the $\text{K-O}_{\text{inner}}$ bonds with
298 increasing temperature as observed by neutron diffraction and X-ray diffraction
299 (Guggenheim *et al.* 1987; Mookherjee *et al.* 2011; Gemmi *et al.* 2008). The K-O
300 vibration does not change after $600\text{ }^{\circ}\text{C}$, indicating K-O bond no longer lengthens.
301 Guggenheim *et al.* (1987) proposed that dehydroxylation in muscovite started with
302 lengthening of K-O2 relative to the other two interlayer bonds, thus this discontinuity
303 in lengthening of K-O bond may be precursory to thermal decomposition or
304 dehydroxylation of the phengite.

305 The broad and overlapping bands of ammonium at high temperatures suggest
306 ordering of ammonium does not occur during heating. In addition, because of thermal
307 expansion of the interlayer sites and lengthening of K-O bonds, hydrogen bonding
308 between ammonium and silicate framework at high temperatures would be negligible.
309 However, hydrogen bonding can appear under low temperatures such as $-150\text{ }^{\circ}\text{C}$
310 stated above because the interlayer distance decreases leading to an increased
311 interaction between ammonium and silicate framework.

312 Previous studies suggested that positive frequency shift with increasing pressure
313 typically indicate an increase in bond strength generated by compression, while
314 negative frequency shift with increasing pressure in hydrogen stretching vibrations are
315 associated with increases in hydrogen bonding (and hence weakening of the primary
316 anion-H bond) (e.g., Cynn and Hofmeister 1994; Vennari *et al.* 2016). In contrast to

317 pressure-induced frequency shift, negative shift of frequency with increasing
318 temperature in vibration spectra typically indicates a weakening in bond strength
319 generated by expansion, while positive shift of frequency of hydrogen stretching
320 vibrations with increasing temperature is associated with weakening hydrogen
321 bonding (and hence strengthening of the primary anion-H bond) (Aines and Rossman
322 1985; Xu et al. 2013; Yang et al. 2015; Thompson et al. 2016). Thus, under low
323 temperatures, the positive frequency shift of N-H stretching band with increasing
324 temperature may indicate hydrogen bonding is the dominant effect. With increasing
325 temperature, hydrogen bond weakens, thereby N-H strengthens. With increasing
326 temperatures above 20 °C, hydrogen bond is too weak to be the dominant effect.
327 Therefore, at high temperatures, the negative frequency shift of N-H stretching
328 vibration with increasing temperature from 20 to 500 °C indicates that lengthening of
329 N-H bond rather than hydrogen bonding is the dominant effect. On further heating
330 above 500 °C, the N-H stretching frequency remains stable, suggesting that the N-H
331 bond no longer lengthens. The bending vibration of ammonium exhibits the similar
332 high temperature behavior with a discontinuity at 400 °C. This probably accounts for
333 the occurrence of the new OH band at 3425 cm⁻¹ during heating, with H transferring
334 from N to the adjacent O and forming O-H. The proton transferring process is
335 reversible with H transferring from O back to N after being quenched.

336 **Mechanism of ammonium loss in phengite**

337 In our experiment, loss of ammonium in phengite starts at 800 °C and is
338 synchronized with dehydration. The results of the present study are consistent with
339 Zhang et al. (2010) and support their conclusion that ammonium loss in muscovite
340 took place at temperatures near dehydration. Based on the above discussion about
341 evolutions of K-O and ammonium bonds with temperatures and origin of the new OH
342 band, we propose the processes involved in ammonium loss illustrated in Figure 10.
343 With increasing temperature, the N-H interatomic distance of NH₄⁺ lengthens until
344 500 °C. N-H bond subsequently no longer lengthens, accompanied by H transferring
345 from N to neighboring O (likely a basal oxygen in the Si₆O₈ ring) and forming a new

346 OH band at 3425 cm^{-1} . The process is reversible and ammonium does not dissociate
347 until the temperature is increased to $800\text{ }^{\circ}\text{C}$. At $800\text{ }^{\circ}\text{C}$, H^{+} starts breaking from N,
348 leaving others forming NH_3 and OH^{-} , just similar to the decomposition of
349 NH_4 -analcime ($\text{NH}_4^{+} + \text{O}_2^{-} = \text{NH}_3 + \text{OH}^{-}$) and NH_4Cl ($\text{NH}_4^{+} + \text{Cl}^{-} = \text{NH}_3 + \text{HCl}$)
350 (Likhacheva et al. 2004; Schmidt and Watenphul 2010). Unfortunately, we did not
351 observe the band of NH_3 vibrations in the IR spectra at high temperatures because of
352 the trace amounts of ammonium in phengite and the open system. However,
353 Likhacheva et al. (2004) indeed found the band around 1626 cm^{-1} of NH_3 in high
354 temperature IR spectra of NH_4 -analcime. Schmidt and Watenphul (2010) also
355 observed the formation of NH_3 at high temperatures based on the appearance of the
356 band around 3310 cm^{-1} in the high temperature Raman spectra of NH_4Cl .
357 Conclusively, the results of our study suggest that the first step of NH_4^{+} loss in
358 phengite corresponds to the following reaction: $\text{NH}_4^{+} + \text{O}^{2-} = \text{NH}_3 + \text{OH}^{-}$, which is
359 consistent with the mechanism proposed for degassing of NH_4 -analcime (Likhacheva
360 et al. 2004).

361 Concerning the products of thermal decomposition of NH_4^{+} in minerals, some
362 studies reported NH_3 (e.g., Weeks et al. 1975; Beyer et al. 1977; Likhacheva et al.
363 2004), while other experiments obtained no NH_3 but N_2 in the products (e.g., Whelan
364 et al. 1988). Haendel et al. (1986) suggested a second process of further conversion of
365 NH_3 to N_2 at elevated temperatures and thus explained the controversy. For the
366 thermal decomposition of NH_3 to N_2 , it follows the slightly endothermic reaction
367 (Cheddie 2012): $2\text{NH}_3 + 94.2\text{ KJ} = \text{N}_2 + 3\text{H}_2$. Thus NH_3 is not stable at high
368 temperatures and begins to decompose at $200\text{ }^{\circ}\text{C}$ (Lan et al. 2012) from
369 thermodynamic analysis. However, the reaction rate depends on temperature as well
370 as catalysts. According to the rate of reaction with catalyst at $800\text{ }^{\circ}\text{C}$ (Li et al. 2009),
371 the fraction of remaining NH_3 was up to 90% after heating for one hour. In this study,
372 no catalyst was introduced during the heating process and the dwelling time was at
373 most 30 minutes at $800\text{ }^{\circ}\text{C}$. As a result, under the conditions of the present study, the
374 second step is not involved and the product of NH_4^{+} decomposition in phengite is

375 most likely dominated by NH_3 . Previous spectroscopic study on NH_4^+ in fluid (NH_4Cl)
376 also showed that a significant amount of NH_4^+ was converted to NH_3 at high
377 temperatures (Schmidt and Watenphul 2010).

378 Although NH_3 is the product of the first step of NH_4^+ decomposition in minerals,
379 the second step involving NH_3 decomposition to N_2 hence could potentially be
380 efficient in natural environment and at geological time scales, because of the existing
381 abundance of catalysts (e.g., Fe_2O_3 , CuO , CaO , ZnO , MnO_2 , TiO_2 , SiO_2 , V_2O_5 , etc.) in
382 geological conditions. This is witnessed for instance by the observation that several
383 high temperature metamorphic rocks are compatible with a release of N_2 rather than
384 NH_3 (e.g., Duit et al. 1986; Bebout and Fogel 1992; Svensen et al. 2008). These
385 effects of catalysts and temperature should be tested further in future experimental
386 studies, specifically exploring variable parameters affecting NH_4^+ fate in high
387 temperature systems.

388 **IMPLICATIONS**

389 From the results obtained herein by IR and Raman spectroscopic analysis of
390 phengite at different temperatures, the following conclusions can be drawn. (1)
391 Dehydration and loss of ammonium in phengite start at the same temperature of
392 800 °C. (2) The mechanism of NH_4^+ loss involves the following process: during
393 heating, the N-H interatomic distance of NH_4^+ lengthens until 500 °C and
394 subsequently no longer lengthens accompanied by H transferring from N to O and
395 forming a new OH band at 3425 cm^{-1} . The process is reversible and ammonium does
396 not dissociate until 800 °C. At 800 °C, H^+ starts breaking from N, leaving others
397 forming NH_3 following the reaction: $\text{NH}_4^+ + \text{O}^{2-} = \text{NH}_3 + \text{OH}^-$.

398 The results of this study imply that phengite cannot preserve a large amount of
399 NH_4^+ in its structure under high temperature conditions (i.e. > 700 °C) even in Ar
400 atmosphere. This finding is in good agreement with general observation that samples
401 subducted along high geothermal gradients experienced drastic N devolatilization
402 with increasing metamorphic conditions, while samples from cooler subduction zones

403 retained N (Bebout and Fogel 1992; Mingram and Bräuer 2001; Busigny et al. 2003a;
404 Elkins et al. 2006; Mitchell et al. 2010; Plessen et al. 2010). The strong temperature
405 dependence of N content during metamorphism was also illustrated by previous work
406 in continental geological settings. For instance, studies on mica-bearing
407 metasediments heated by granitic intrusion demonstrated that bulk-rock N content
408 decreased along a profile toward the granite contact (e.g., Bebout et al. 1999b; Jia
409 2006). Nitrogen was released at temperature higher than ~500 °C, which is slightly
410 lower than the temperature identified in the present laboratory experiment. The
411 distinct temperatures of N devolatilization may reflect that (1) natural metasediments
412 are not made of a single N-bearing mineral (i.e. phengite in the present experiment)
413 but correspond to complex matrixes including muscovite, biotite, and K-feldspars, or
414 that (2) a kinetic effect controls partly NH_4^+ destabilization in micas since
415 metasediments were left at high temperature over geological timescale (several Ma),
416 which contrasts with the 30 minutes of the present experiment. Longer laboratory
417 experiments should be designed to test this possibility. Finally, to further address the
418 N cycle in deep Earth, kinetics of NH_4^+ loss in phengite and other NH_4^+ -bearing
419 minerals in the mantle (e.g., clinopyroxene) need to be investigated in future work.

420

ACKNOWLEDGMENTS

421 This work was supported by the Fundamental Research Funds for the Central
422 Universities (2016QNA3014). Vincent Busigny was funded by the Research Program
423 SYSTER-2012 of the Institut National des Sciences de l'Univers. Comments and
424 suggestions from two anonymous reviewers helped to improve the manuscript. The
425 authors also warmly thank Warren Huff for editing the manuscript.

426

REFERENCES

427 Aines, R.D. and Rossman, G.R. (1985) The high temperature behavior of trace
428 hydrous components in silicate minerals. *American Mineralogist*, 70: 1169-1179.
429 Bebout, G.E. and Fogel, M. (1992) Nitrogen-isotope compositions of

- 430 metasedimentary rocks in the Catalina Schist, California: Implications for
431 metamorphic devolatilization history. *Geochimica et Cosmochimica Acta*, 56:
432 2839-2849.
- 433 Bebout, G.E., Ryan, J.G., Leeman, W.P, and Bebout, A.E. (1999a) Fractionation of
434 trace elements by subduction-zone metamorphism-effect of convergent-margin
435 thermal evolution. *Earth and Planetary Science Letters*, 171: 63-81.
- 436 Bebout G.E., Cooper D.C., Don Bradley A., and Sadofsky S.J. (1999b)
437 Nitrogen-isotope record of fluid-rock interactions in the Skiddaw Aureole and
438 granite, English Lake District. *American Mineralogist*, 84: 1495-1505.
- 439 Bebout, G.E., Lazzeri, K.E., and Geiger, C.A. (2016) Pathways for nitrogen cycling in
440 Earth's crust and upper mantle: A review and new results for microporous beryl
441 and cordierite. *American Mineralogist*, 101: 7-24.
- 442 Beyer, H.K., Jacobs, P.A., Uytterhoeven, J.B., and Till, F. (1977) Thermal stability of
443 NH₄-chabazite. *Journal of the Chemical Society Faraday Transactions*, 73:
444 1111-1118.
- 445 Buback, M. and Schulz, K.R. (1976) Raman Scattering of Pure Ammonia to High
446 Pressures and Temperatures. *Journal of Physics and Chemistry*, 80: 2478-2482.
- 447 Busigny, V., Cartigny, P., Philippot, P., Ader, M., and Javoy, M. (2003a) Massive
448 recycling of nitrogen and other fluid-mobile elements (K, Rb, Cs, H) in a cold
449 slab environment: evidence from HP to UHP oceanic metasediments of the
450 Schistes Lustrés nappe (western Alps, Europe). *Earth and Planetary Science
451 Letters*, 215: 27-42.
- 452 Busigny, V., Cartigny, P., Philippot, P., and Javoy, M. (2003b) Ammonium
453 quantification in muscovite by infrared spectroscopy. *Chemical Geology*, 198:
454 21-31.
- 455 Busigny, V. and Bebout, G.E. (2013) Nitrogen in the silicate Earth: Speciation and
456 isotopic behavior during mineral-fluid interactions. *Elements*, 9: 353-358.

- 457 Cartigny, P. and Marty, B. (2013) Nitrogen isotopes and mantle geodynamics: The
458 emergence of life and the atmosphere-crust-mantle connection. *Elements*, 9:
459 359-366.
- 460 Cheddie, D. (2012) Ammonia as a hydrogen source for fuel cells: a review. In: Minic,
461 D., Ed., *Hydrogen Energy-Challenges and Perspectives*, Intech, Rijeka, 333-362.
- 462 Cynn, H. and Hofmeister, A.M. (1994) High-pressure IR spectra of lattice modes and
463 OH vibrations in Fe-bearing wadsleyite. *Journal of Geophysical Research*, 99:
464 17717-17727.
- 465 Domanik, K.J. and Holloway, J.R. (1996) The stability and composition of phengitic
466 muscovite and associated phases from 5.5 to 11 GPa: Implications for deeply
467 subducted sediments. *Geochimica et Cosmochimica Acta*, 60: 4133-4150.
- 468 Duit, W., Jansen, J.B.H., van Breeman, A., and Bos, A. (1986) Ammonium micas in
469 metamorphic rocks as exemplified by Dome de L'Agout (France). *American
470 Journal of Science*, 286: 702-732.
- 471 Elkins, L., Fischer, T., Hilton, D., Sharp, Z., McKnight, S., and Walker, J. (2006)
472 Tracing nitrogen in volcanic and geothermal volatiles from the Nicaraguan
473 volcanic front. *Geochimica et Cosmochimica Acta*, 70: 5125-5235.
- 474 Galloway, J.N. (2003) The global nitrogen cycle. In *Treatise on Geochemistry*,
475 chapter 8.12, p. 557-583. Elsevier, Amsterdam.
- 476 Gemmi, M., Merlini, M., Pavese, A., and Curetti, N. (2008) Thermal expansion and
477 dehydroxylation of phengite micas. *Physics and Chemistry of Minerals*, 35:
478 367-379.
- 479 Guggenheim, S., Chang, Yu-H., and Koster van Groos, A.F. (1987) Muscovite
480 dehydroxylation: High-temperature studies. *American Mineralogist*, 72: 537-550.
- 481 Goldblatt, C., Claire, M.W., Lenton, T.M., Matthews, A.J., Watson, A.J., and Zahnle,
482 K.J. (2009) Nitrogen enhanced greenhouse warming on early Earth. *Nature
483 Geoscience*, 2: 891-896.

- 484 Halama, R., Bebout, G.E., John, T., and Scambelluri, M. (2014) Nitrogen recycling in
485 subducted mantle rocks and implications for the global nitrogen cycle.
486 International Journal of Earth Sciences (Geol Rundsch), 103: 2081-2099.
- 487 Haendel, D., Muhle, K., Nitzsche, H.M., Stiehl, G., and Wand, U. (1986) Isotopic
488 variations of the fixed nitrogen in metamorphic rocks. Geochimica et
489 Cosmochimica Acta, 50: 749-758.
- 490 Harlov, D.E., Andrut, M., and Pöter, B. (2001) Characterization of buddingtonite
491 (NH₄)(AlSi₃O₈) and ND₄-buddingtonite (ND₄)(AlSi₃O₈) using IR spectroscopy
492 and Rietveld refinement of XRD spectra. Physics and Chemistry of Minerals, 28:
493 188-198.
- 494 Herzberg, G. (1966) Molecular spectra and molecular structure Vol.2: Infrared and
495 Raman spectra of polyatomic molecules. Van Nostrand, Princeton.
- 496 Higashi, S. (1978) Dioctahedral mica minerals with ammonium ions. Journal of
497 Mineralogical and Petrological, 9: 16-27.
- 498 Higashi, S. (2000) Ammonium-bearing mica and mica/smectite of several pottery
499 stone and pyrophyllite deposits in Japan: Their mineralogical properties and
500 utilization. Applied Clay Science, 16: 171-184.
- 501 Holtz, M., Solin, S.A., and Pinnavaia, T.J. (1993) Effect of pressure on the Raman
502 vibrational modes of layered aluminosilicate compounds. Physical Review B,
503 13313-13317.
- 504 Ivaldi, G., Ferraris, G., Guretti, N., and Compagnoni, R. (2001) Coexisting 3T and
505 2M₁ polytypes of phengite from Cima Pal (Val Savenca, western Alps):
506 Chemical and polytypic zoning and structural characterization. European Journal
507 of Mineralogy, 13: 1025-1034.
- 508 Jia Y. (2006) Nitrogen isotope fractionations during progressive metamorphism: A
509 case study from the Paleozoic Cooma metasedimentary complex, southeastern
510 Australia. Geochimica et Cosmochimica Acta, 70: 5201-5214.

- 511 Johnson, B. and Goldblatt, C. (2015) The nitrogen budget of Earth. *Earth-Science*
512 *Reviews*, 148: 150-173.
- 513 Kearley, G.J. and Oxtun, L.A. (1983) Recent advances in the vibrational spectroscopy
514 of ammonium ion in crystal. In R.J.H. Clark and R.E. Hesters, Eds., *Advances in*
515 *Infrared and Raman Spectroscopy*, 10, Chapter 2. John Wiley and Sons, New
516 York.
- 517 Lan, R., Irvine, J.T.S., and Tao, S. (2012) Ammonia and related chemicals as potential
518 indirect hydrogen storage materials. *International Journal of Hydrogen Energy*,
519 37: 1482-1494.
- 520 Li, L., Cartigny, P., and Ader, M. (2009) Kinetic nitrogen isotope fractionation
521 associated with thermal decomposition of NH₃: Experimental results and
522 potential applications to trace the origin of N₂ in natural gas and hydrothermal
523 systems. *Geochimica et Cosmochimica Acta*, 73: 6282-6297.
- 524 Li, L., Zheng, Y.F., Cartigny, P., and Li, J. (2014) Anomalous nitrogen isotopes in
525 ultrahigh-pressure metamorphic rocks from the Sulu orogenic belt: Effect of
526 abiotic nitrogen reduction during fluid-rock interaction. *Earth and Planetary*
527 *Science Letters*, 403: 67-78.
- 528 Li, Y., Wiedenbeck, M., Shcheka, S., and Keppler, H. (2013) Nitrogen solubility in
529 upper mantle minerals. *Earth and Planetary Science Letters*, 377: 311-323.
- 530 Likhacheva, A.Y., Veniaminov, S.A., and Paukshtis, E.A. (2004) Thermal
531 decomposition of NH₄-analcime. *Physics and Chemistry of Minerals*, 31:
532 306-312.
- 533 McKeown, D.A., Bell, M.L., and Etz, E. (1999) Vibrational analysis of the
534 dioctahedral mica: 2M1 muscovite. *American Mineralogist*, 84: 1041-1048.
- 535 Mikhail, S. and Sverjensky, D.A. (2014) Nitrogen speciation in upper mantle fluids
536 and the origin of Earth's nitrogen-rich atmosphere. *Nature Geoscience*, 7:
537 816-819.

- 538 Mingram, B. and Bräuer, K. (2001) Ammonium concentration and nitrogen isotope
539 composition in metasedimentary rocks from different tectonometamorphic units
540 of the European Variscan Belt. *Geochimica et Cosmochimica Acta*, 65: 273-287.
- 541 Miroshnichenko, Y.M. and Drebuschak, V.A. (2003) Thermal decomposition of
542 NH₄-analcime: A kinetic study. *Geophysical Research Abstract*, vol. 5, 00298
543 (European Geophysical Society 2003).
- 544 Mitchell, E.C., Fischer, T.P., Hilton, D.R., Hauri, E.H., Shaw, A.M., de Moor, J.M.,
545 Sharp, Z.D., and Kazahaya, K. (2010) Nitrogen sources and recycling at
546 subduction zones: Insights from the Izu-Bonin-Mariana arc. *Geochemistry
547 Geophysics Geosystems*, 11: 1448-1470.
- 548 Mookherjee, M., Redfern, S.A.T., and Zhang, M. (2001) Thermal response of
549 structure and hydroxyl ion of phengite 2M1: an in situ neutron diffraction and
550 FTIR study. *European Journal of Mineralogy*, 13: 545-555.
- 551 Mookherjee, M. and Redfern, S.A.T. (2002) A high-temperature Fourier transform
552 infrared study of the interlayer and Si-O-stretching region in phengite-2M₁. *Clay
553 Minerals*, 37: 323-336.
- 554 Mookherjee, M., Redfern, S.A.T., Zhang, M., and Harlov, D.E. (2002a) Orientational
555 order-disorder in synthetic ND₄/NH₄-phlogopite: a low-temperature infrared
556 study. *European Journal of Mineralogy*, 14: 1033-1039.
- 557 Mookherjee, M., Redfern, S.A.T., Zhang, M., Harlov, and D.E. (2002b) Orientational
558 order-disorder of N(D,H)₄⁺ in tobelite. *American Mineralogist*, 87: 1686-1691.
- 559 Nobel, S.M. (2016) Solubility of nitrogen in stishovite: A possible storage mechanism
560 for nitrogen in Earth's deep interior: [D]. Arizona State University.
- 561 Okumura, S. and Nakashima, S. (2005) Molar absorptivities of OH and H₂O in
562 rhyolitic glass at room temperature and at 400-600 °C. *American Mineralogist*,
563 90: 441-447.
- 564 Palya, A.P., Buick, I.S., and Bebout, G.E. (2011) Storage and mobility of nitrogen in

- 565 the continental crust: Evidence from partially melted metasedimentary rocks, Mt.
566 Stafford, Australia. *Chemical Geology*, 281: 211-226.
- 567 Pauling, L. (1930) Rotational motion of molecules in crystals. *Physics Review*, 36:
568 430-443.
- 569 Plessen, B., Harlov, D.E., Henry, D., and Guidotti C.V. (2010) Ammonium loss and
570 nitrogen isotopic fractionation in biotite as a function of metamorphic grade in
571 metapelites from western Maine, USA. *Geochimica et Cosmochimica Acta*, 74:
572 4759-4771.
- 573 Plumb, R.C. and Hornig, D.F. (1950) Infrared spectrum, X-ray diffraction pattern, and
574 structure of ammonium fluoride. *The Journal of Physical Chemistry*, 23:
575 947-953.
- 576 Poli, S. and Schmidt, M.W. (1995) H₂O transport and release in subduction
577 zones-experimental constraints on basaltic and andesitic systems. *Journal of*
578 *Geophysical Research*, 100: 22299-314.
- 579 Reed, J.W. and Williams, Q. (2006) An infrared spectroscopic study of NH₄Br-
580 ammonium bromide to 55 GPa. *Solid State Communications*, 140: 202-207.
- 581 Schmidt, C. and Watenphul, A. (2010) Ammonium in aqueous fluids to 600°C, 1.3
582 GPa: A spectroscopic study on the effects on fluid properties, silica solubility,
583 and K-feldspar to muscovite reactions. *Geochimica et Cosmochimica Acta*, 74:
584 6852-6866.
- 585 Schmidt, M.W. (1996) Experimental constraints on recycling of potassium from
586 subducted ocean crust. *Science*, 272: 1972-1930.
- 587 Schmidt, M.W. and Poli, S. (1998) Experimentally based water budgets for
588 dehydrating slabs and consequences for arc magma generation. *Earth and*
589 *Planetary Science Letters*, 163: 361-379.
- 590 Schmidt, M.W. and Poli, S. (2014) Devolatilization during subduction. In R.L. Rud-
591 nick, Ed., *Treatise on Geochemistry: The Crust*, 2nd ed., 3, p. 669-701. Elsevier,

- 592 Amsterdam.
- 593 Svensen, H., Bebout, G.E., Kronz, A., Li, L., Planke, S., Chevallier, L., and Jamtveit,
594 B. (2008) Nitrogen geochemistry as a tracer of fluid flow in a hydrothermal vent
595 complex in the Karoo Basin, South Africa. *Geochimica et Cosmochimica Acta*,
596 72: 4929-4947.
- 597 Tateyama, H., Shimda, S., and Sudo, T. (1977) Estimation of K-O distance and
598 tetrahedral rotation angle of K-micas from far-infrared absorption spectral data.
599 *American Mineralogist*, 62: 534-539.
- 600 Thompson, E.C., Campbell, A.J., and Liu, Z. (2016) In-situ infrared spectroscopic
601 studies of hydroxyl in amphiboles at high pressure. *American Mineralogist*, 101:
602 706-712.
- 603 Tokiwai, K. and Nakashima, S. (2010) Integral molar absorptivities of OH in
604 muscovite at 20 to 650 °C by in-situ high-temperature IR microspectroscopy.
605 *American Mineralogist*, 95: 1052-1059.
- 606 Vedder, W. (1965) Ammonium in muscovite. *Geochimica et Cosmochimica Acta*, 29:
607 221-228.
- 608 Vennari, C.E., O'Bannon, E.F., and Williams, Q. (2016) The ammonium ion in a
609 silicate under compression: infrared spectroscopy and powder X-ray diffraction
610 of $\text{NH}_4\text{AlSi}_3\text{O}_8$ -buddingtonite to 30 GPa. *Physics and Chemistry of Minerals*,
611 DOI 10.1007/s00269-016-0844-3.
- 612 Watenphul, A., Wunder, B., and Heinrich, W. (2009) High-pressure
613 ammonium-bearing silicates: implications for nitrogen and hydrogen storage in
614 the Earth's mantle. *American Mineralogist*, 94: 283-292.
- 615 Watenphul, A., Wunder, B., Wirth, R., and Heinrich, W. (2010) Ammonium-bearing
616 clinopyroxene: A potential nitrogen reservoir in the Earth's mantle. *Chemical
617 Geology*, 270: 240–248.
- 618 Weeks, T.J., Angell, C.L., and Bolton, A.P. (1975) The thermochemical properties of

- 619 ammonium exchanged erionite. *Journal of Catalysis*, 38: 461-468.
- 620 Whelan, J.K., Solomon, P.R., Desphande, G.V., and Carangelo, R.M. (1988)
621 Thermogravimetric Fourier transform infrared spectroscopy (TG-FTIR) of
622 petroleum source rocks-initial results. *Energy & Fuels*, 2: 65-73.
- 623 Williams, L.B., Wilcoxon, B.R., Ferrell, R.E., and Sassen, R. (1992) Diagenesis of
624 ammonium during hydrocarbon maturation and migration, Wilcox Group,
625 Louisiana, USA. *Applied Geochemistry*, 7: 123-134.
- 626 Williams, Q., Knittle, E., Scott, H.P., and Liu, Z.X. (2012) The high--pressure
627 behavior of micas: Vibrational spectra of muscovite, biotite, and phlogopite to 30
628 GPa. *American Mineralogist*, 97: 241-252.
- 629 Wunder, B., Berryman, E., Plessen, B., Rhede, D., Koch-Müller, M., and Heinrich, W.
630 (2015) Synthetic and natural ammonium-bearing tourmaline. *American*
631 *Mineralogist*, 100: 250-256.
- 632 Xu, H., Zhao, Y., Hickmott, D.D., Lane, N.J., Vogel, S.C., Zhang, J., and Daemen,
633 L.L. (2013): High-temperature neutron diffraction study of deuterated brucite.
634 *Physics and Chemistry of Minerals*, 40: 799-810.
- 635 Yang, Y., Xia, Q.K., Feng, M., and Zhang, P.P. (2010) Temperature dependence of IR
636 absorption of OH species in clinopyroxene. *American Mineralogist*, 95:
637 1439-1443.
- 638 Yang, Y., Xia, Q.K., Feng, M., and Liu, S.C. (2012) OH in nature orthopyroxene: an
639 in situ FTIR investigation at varying temperatures. *Physics and Chemistry of*
640 *Minerals*, 39: 413-418.
- 641 Yang, Y., Xia, Q.K., and Zhang, P.P. (2015) Evolutions of OH groups in diopside and
642 feldspars with temperature. *European Journal of Mineralogy*, 27: 185-192.
- 643 Yokochi, R., Marty, B., Chazot, G., and Burnard, P. (2009) Nitrogen in peridotite
644 xenoliths: Lithophile behavior and magmatic isotope fractionation. *Geochimica*
645 *et Cosmochimica Acta*, 73: 4843-4861.

646 Zhang, M., Salje, E.K.H., Carpenter, M.A., Wang, J.Y., Groat, L.A., Lager, G.A.,
647 Wang, L., Beran, A., and Bismayer, U. (2007) Temperature dependence of IR
648 absorption of hydrous/hydroxyl species in minerals and synthetic materials.
649 American Mineralogist, 92: 1502-1517.

650 Zhang, M., Redfern, S.T., Salje, E.K.H., Carpenter, M.A., and Hayward, C.L. (2010)
651 Thermal behavior of vibrational phonons and hydroxyls of muscovite in
652 dehydroxylation: In situ high-temperature infrared spectroscopic investigations.
653 American Mineralogist, 95: 1444-1457.

654 Table 1 Assignments of the observed IR and Raman bands in phengite at ambient
655 conditions

ν (cm ⁻¹)	Assignment
104	K-O stretching
192	M2-OH stretch. + Od xz-trans.
270	Ob, OH y-trans. + Oc, e z-trans. + K y-trans.
706	O out-of-plane Trans.+M-O Str.
1430	NH ₄ bending band
2818	overtone antisymmetric bending
3036	combination of NH ₄ symmetric and antisymmetric bending
3291	N-H stretching
3610	O-H stretching
4500	combination (O-H stretching and H-O-Si(Al) bending)

656 Note: The bands are assigned referring to Holtz et al. (1993), McKeown et al. (1999),
657 Mookherjee and Redfern (2002), Busigny et al. (2003b), Zhang et al. (2010) and
658 Williams et al. (2012), Mookherjee et al. (2012a and 2012b).

659 **Figure captions:**

660 Figure 1 The illustration of ammonium in the phengite structure. The crystal structure of phengite
661 of 3T polytype is from Ivaldi et al. (2001).

662 Figure 2 (a) FTIR spectra of phengite (0.112 mm thickness) at room temperature; (b) A detailed
663 view of the deconvolved ammonium bands. The marked bands originate from vibrations of
664 ammonium and OH. The spectra are vertically offset for clarity.

- 665 Figure 3 *In situ* FTIR spectra of phengite (0.125 mm thickness) at low temperatures. Arrows
666 indicates peak splitting at low temperatures. The dotted line is to guide the eye. The spectra
667 are vertically offset for clarity.
- 668 Figure 4 *In situ* FTIR spectra of phengite (0.098 mm thickness) at high temperatures: (a) heating
669 in air; (b) heating in Ar. The blue dotted lines are to show the new OH band appearing with
670 increasing temperature, and the black dotted lines are to show the evolutions ammonium
671 bands with temperature. The spectra are vertically offset for clarity.
- 672 Figure 5 Frequencies of (a) N-H stretching band and (b) bending band in phengite as a function of
673 temperature. The error bars represent standard deviations which are obtained by performing
674 multiple fits on the spectra.
- 675 Figure 6 Time evolution of *in situ* IR spectra of phengite isothermally annealed at (a) 500 °C
676 (using the grain with 0.084 mm thickness) and (b) 700 °C (using the grain with 0.115 mm
677 thickness) in air. The spectra are vertically offset for clarity.
- 678 Figure 7 Room-temperature spectra recorded before and after the isothermal annealing for 30 min
679 at (a) 750 °C (using the grain with 0.03 mm thickness) and (b) 800 °C (using the grain with
680 0.01 mm thickness) in Ar. The spectra are vertically offset for clarity.
- 681 Figure 8 *In situ* Raman spectra of phengite (0.119 mm thickness) at high temperatures. The spectra
682 are vertically offset for clarity.
- 683 Figure 9 Frequency shifts of lattice modes with temperature: (a) the 104 cm⁻¹ band; (b) the 192
684 cm⁻¹ band; (c) the 270 cm⁻¹ band, and (d) 706 cm⁻¹ band. The error bars represent standard
685 deviations which are obtained by performing multiple fits on the spectra.
- 686 Figure 10 Schematic illustration of the mechanism of ammonium loss during the heating process.

Figure 1

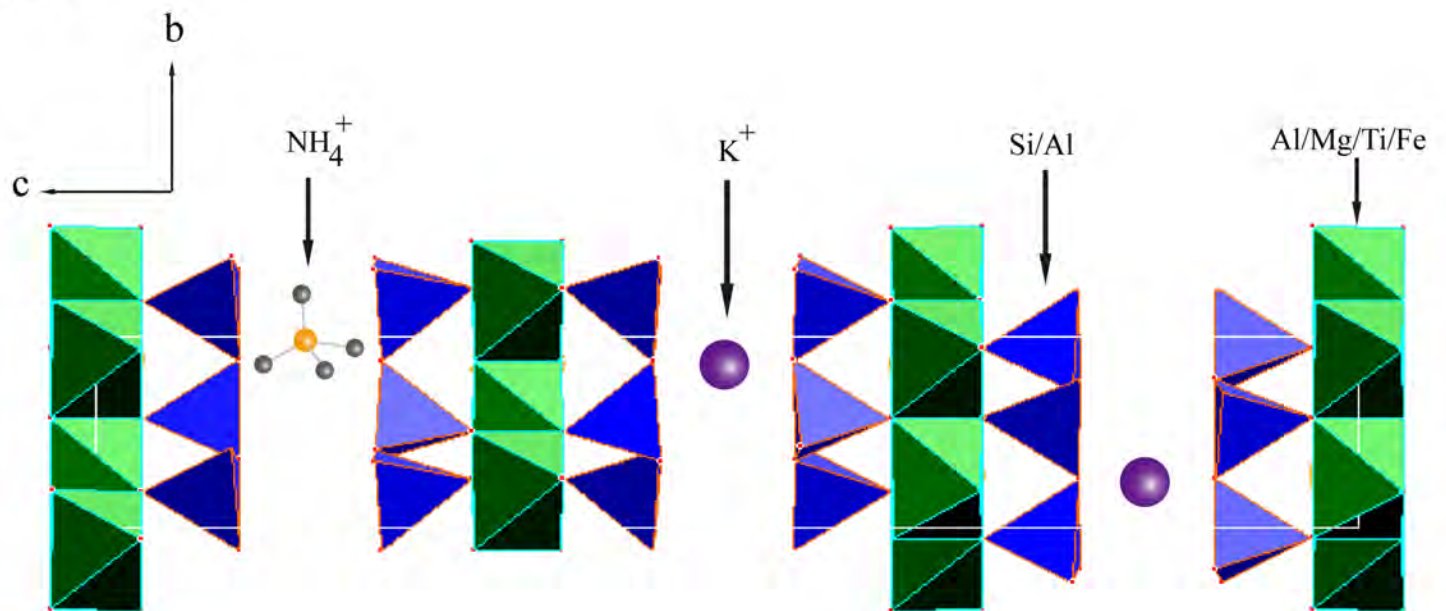


Figure 2

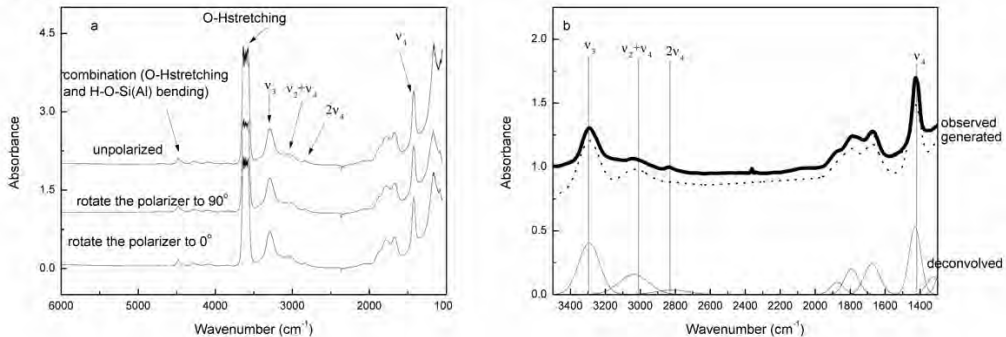


Figure 3

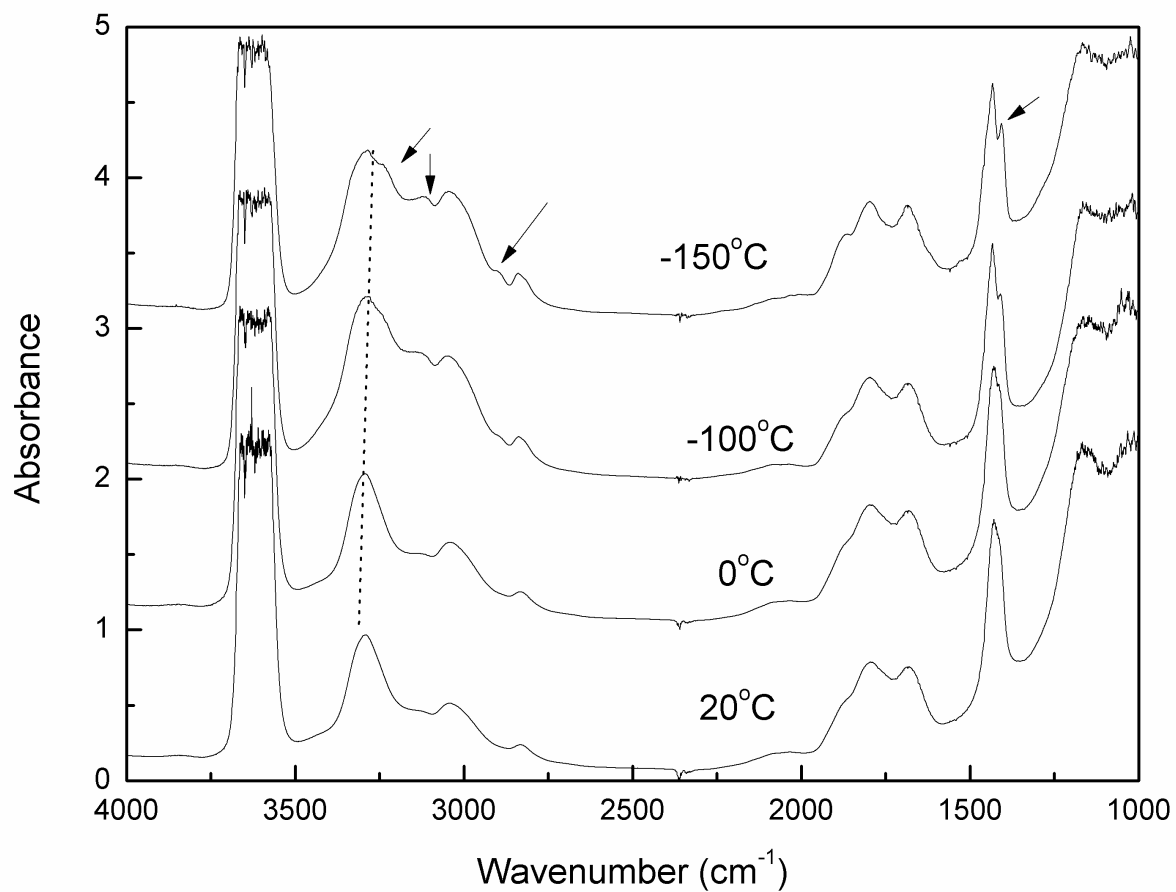


Figure 4

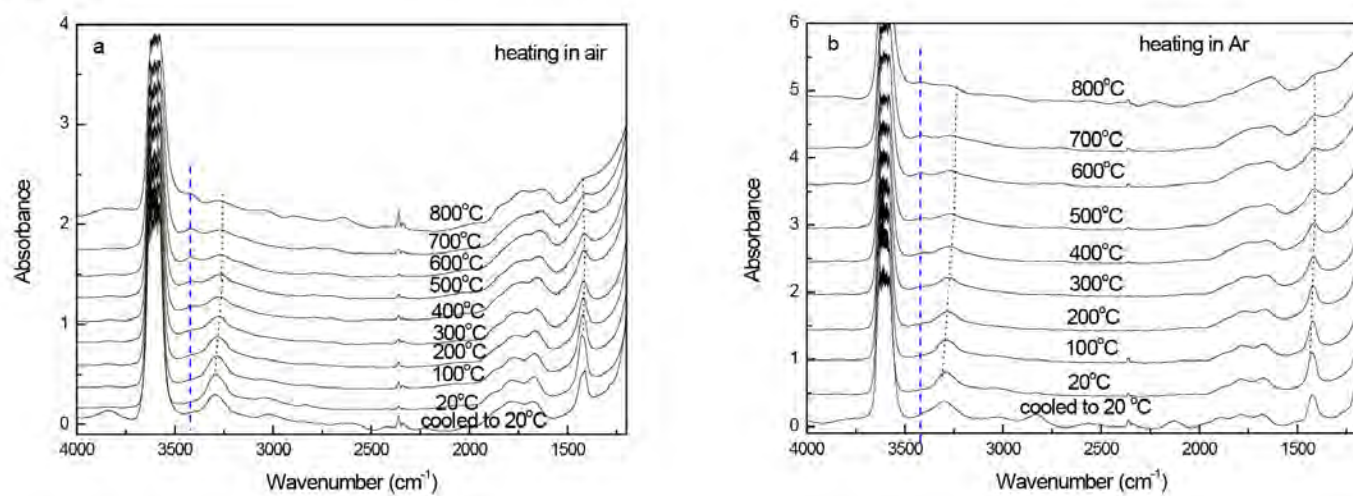


Figure 5

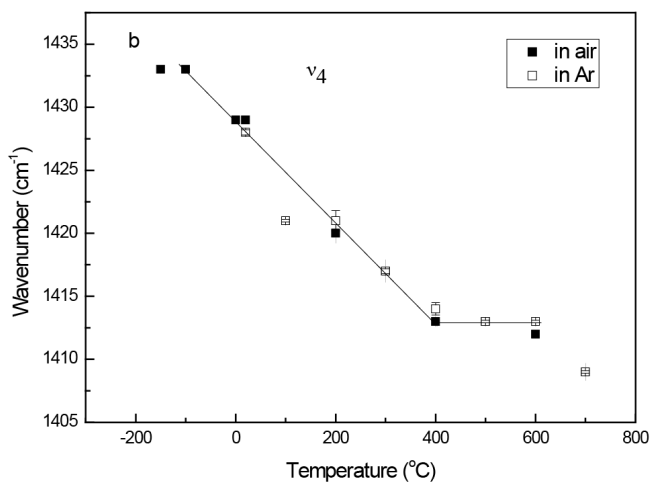
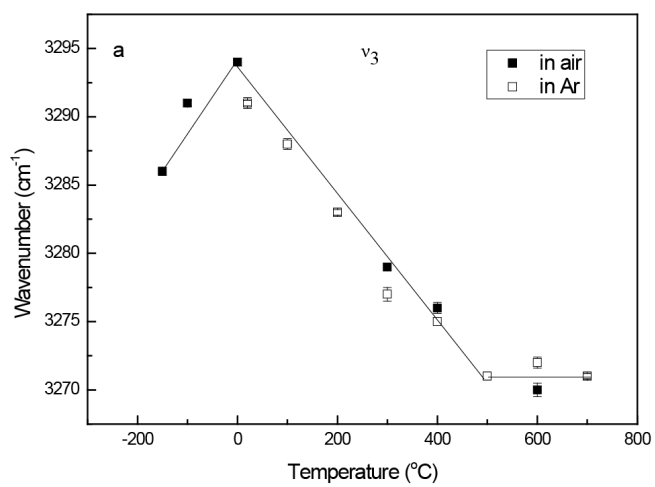


Figure 6

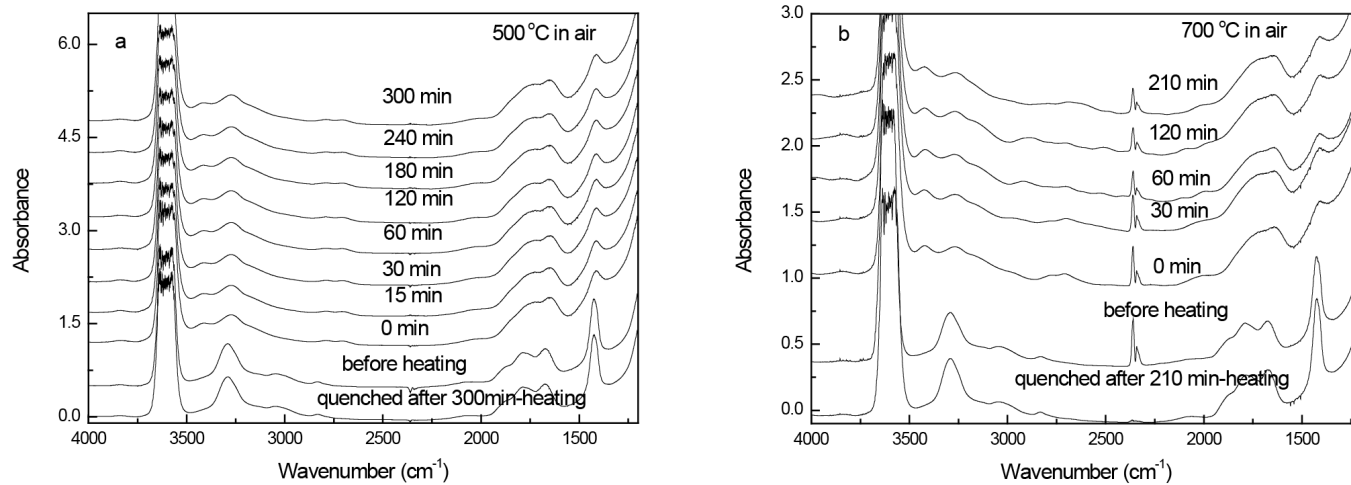


Figure 7

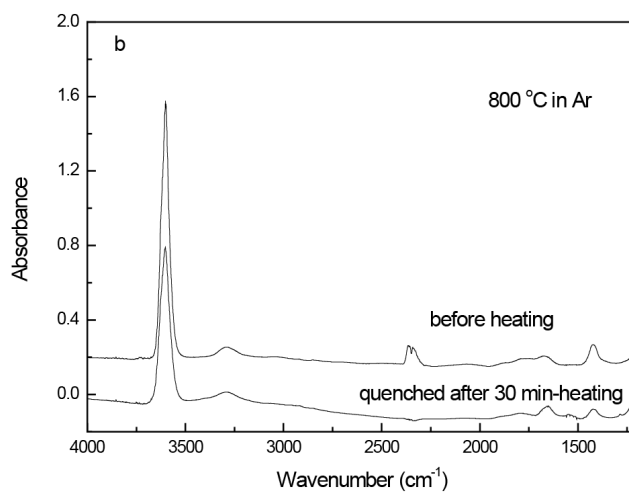
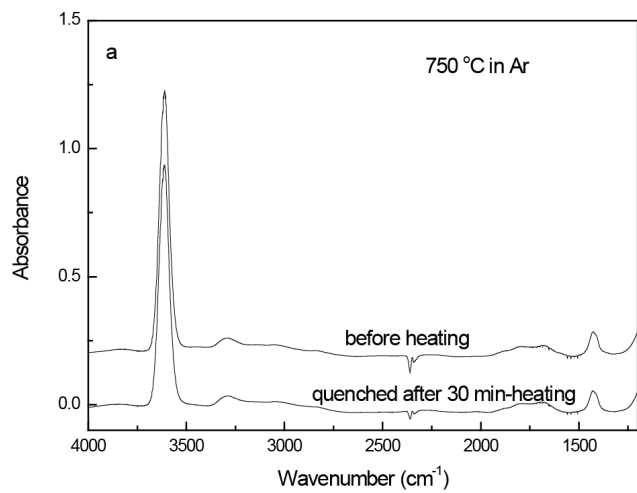


Figure 8

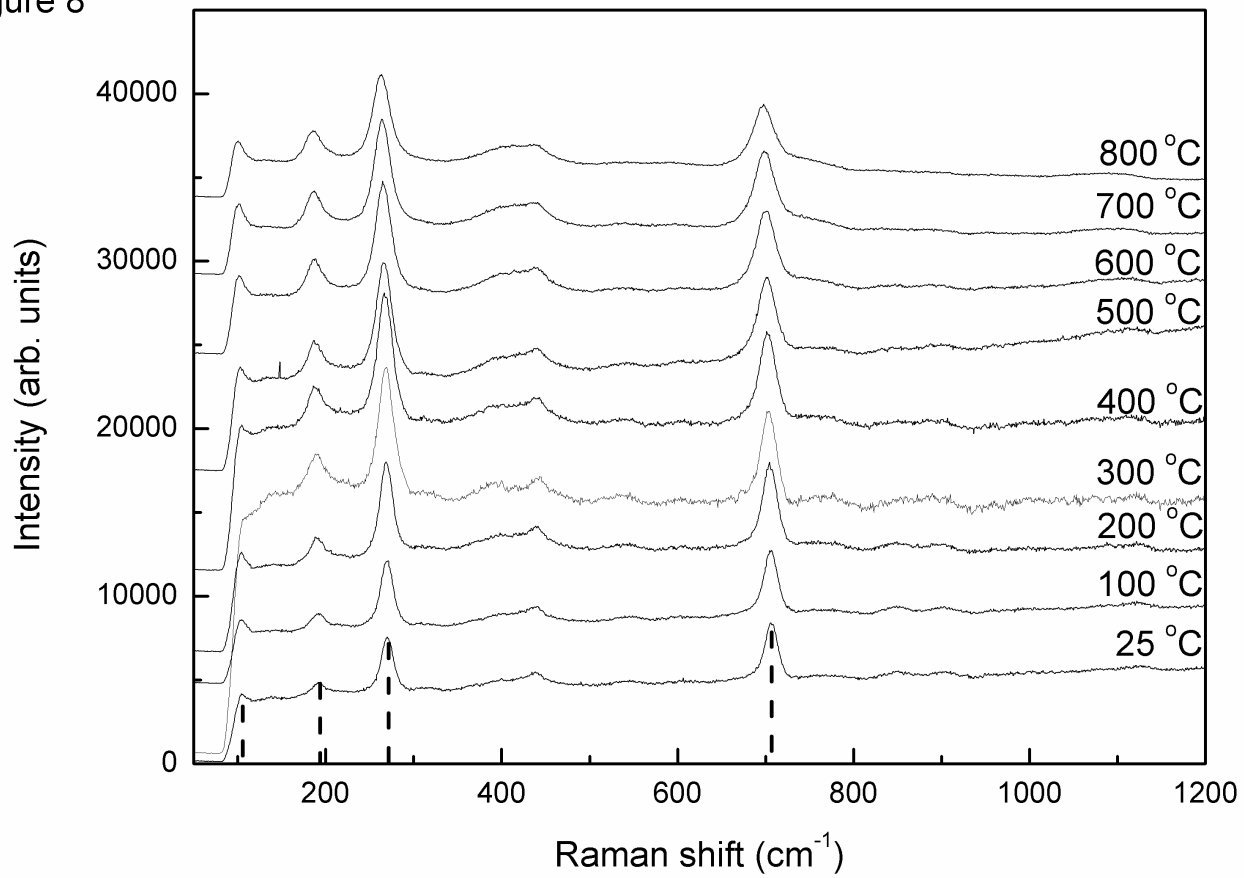


Figure 9

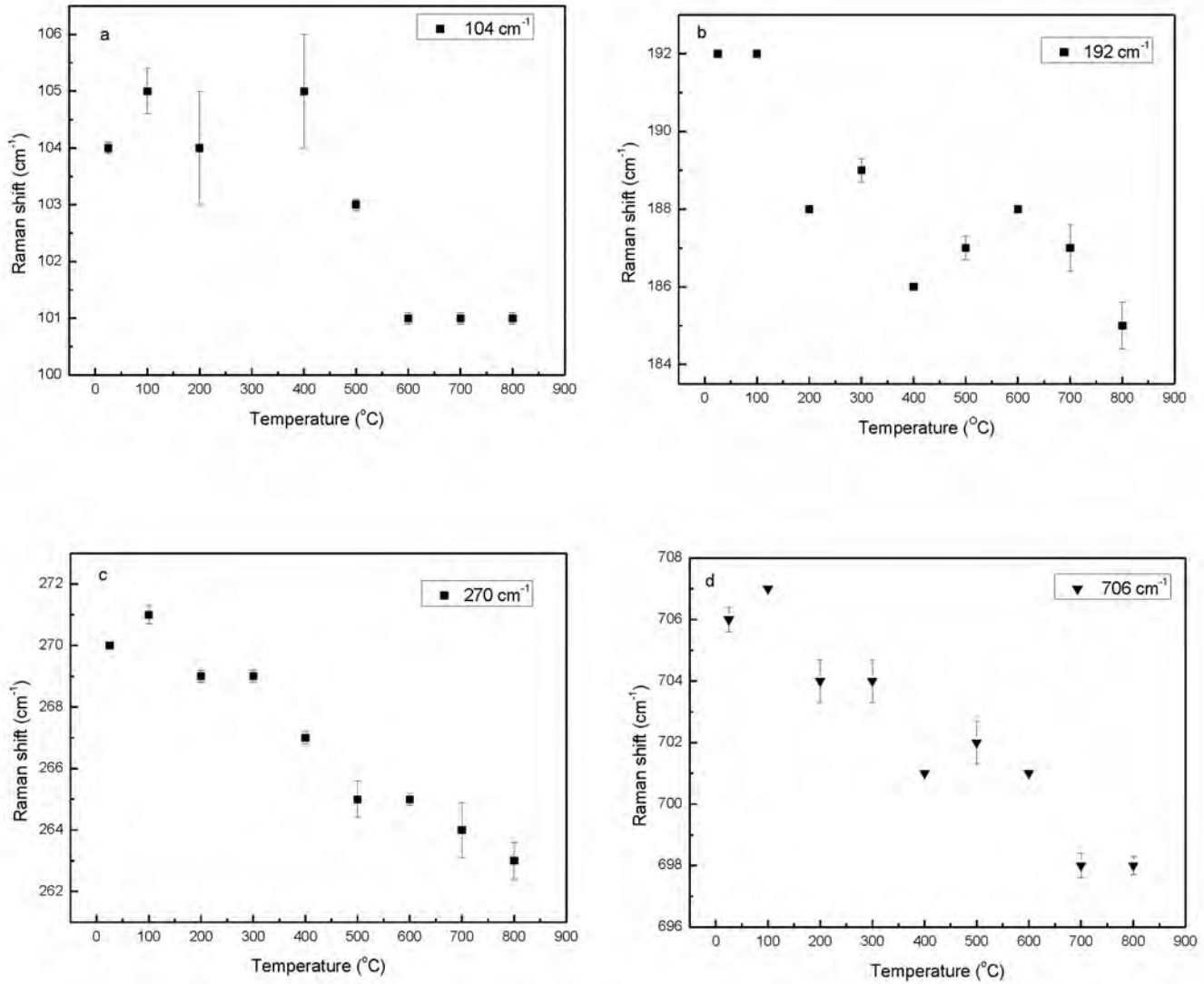


Figure 10

